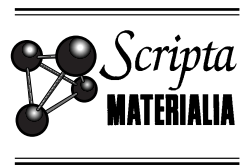




PERGAMON

Scripta mater. 44 (2001) 2357–2361



www.elsevier.com/locate/scriptamat

## MAGNETIC SMALL-ANGLE NEUTRON SCATTERING BY NANOCRYSTALLINE TERBIUM

J. Weissmüller<sup>1,2</sup>, D. Michels<sup>2</sup>, A. Michels<sup>2</sup>, A. Wiedenmann<sup>3</sup>, C.E. Krill<sup>2</sup>,  
H.M. Sauer<sup>2</sup> and R. Birringer<sup>2</sup>

<sup>1</sup>Forschungszentrum Karlsruhe, Institut für Nanotechnologie, Karlsruhe, Germany <sup>2</sup>Universität des Saarlandes, Technische Physik, Saarbrücken, Germany <sup>3</sup>Hahn-Meitner Institut, BENSC, Berlin, Germany

(Received August 21, 2000)

(Accepted in revised form December 15, 2000)

**Abstract**—We present an experimental study of the magnetic microstructure in the nanocrystalline hard magnet Tb. Field-dependent SANS data are analyzed quantitatively in terms of the correlation function of the spin misalignment. We find that up to applied fields of several Tesla the magnetization remains ‘locked in’ to the basal planes of the hcp crystal lattice of each individual crystallite; But that the in-plane orientation of the spins is highly nonuniform within each particle. This internal structure can be suppressed by the applied field. © 2001 Acta Materialia Inc. Published by Elsevier Science Ltd. All rights reserved.

**Keywords:** Magnetic structure; Neutron scattering; Hard magnets

### Introduction

In nanocrystalline ferromagnets the orientation of the magnetization vector is highly nonuniform on the nanometer-scale because at each grain boundary the set of crystallographic ‘easy axes’ for the magnetization changes its orientation. Studying the detailed nature of this nonuniformity is of importance for understanding the dependence of the macroscopic magnetic properties of these materials on the grain size. Micromagnetics computer simulations provide insight into this issue, but there are few experimental data on the magnetic microstructure in the bulk of nanocrystalline ferromagnets. In fact, small-angle neutron scattering (SANS) appears to be the only known technique with a potential to resolve the magnetic microstructure in the bulk and on the length-scales of interest, few nm to few hundred nm. SANS experiments have been carried out on essentially soft magnetic nanocrystalline samples of the elemental transition metals Fe, Ni, and Co (1,2,3,4), and on nanocrystalline soft magnets crystallized from glasses (5). Recently, such data were combined with a general theory for magnetic SANS by ferromagnets near saturation based on a micromagnetics model (6), an approach that supplies quantitative data on the magnetic microstructure, the exchange-stiffness constant, and the magnitude and microstructure of the magnetic anisotropy (4). However, nanocrystalline hard magnets have not previously been studied by SANS. In this paper, we present the first such study, an investigation of nanocrystalline Tb. The data are analyzed in terms of a correlation function of the spin misalignment. We summarize some of the relevant equations (for a detailed derivation see (7), and discuss experimental results and their implications.

### Correlation Function and Correlation Length

A correlation function,  $C(\mathbf{r})$ , of the spin misalignment can be defined by

$$C(\mathbf{r}) = m_s^{-2} V^{-1} \iiint (\mathbf{M}(\mathbf{x}) - \langle \mathbf{M} \rangle) \cdot (\mathbf{M}(\mathbf{x} + \mathbf{r}) - \langle \mathbf{M} \rangle) d^3x, \quad (1)$$

where  $\mathbf{M}(\mathbf{x})$  represents the magnetization and  $\langle \mathbf{M} \rangle$ ,  $m_s$ , and  $V$  denote, respectively, the macroscopic magnetization, saturation magnetization, and sample volume.  $C(\mathbf{r})$  is related to the Fourier transform  $\mathbf{m}(\mathbf{q})$  of the reduced magnetization,  $(\mathbf{M}(\mathbf{x}) - \langle \mathbf{M} \rangle)/m_s$ , by

$$C(r) = V^{-1} \iiint |\mathbf{m}(\mathbf{q})|^2 \exp(i\mathbf{q}\mathbf{r}) d^3q. \quad (2)$$

A rigorous evaluation of  $C(\mathbf{r})$  may require that the complete information on the orientation and magnitude of the vector  $\mathbf{m}$  as a function of the orientation and magnitude of the wavevector  $\mathbf{q}$  is measured. In general, this immense data base will not be available, but useful information on  $C(\mathbf{r})$  can still be derived from experimental scattering cross-sections. We have evaluated two limiting cases, namely (i) the isotropic case, e.g. a texture-free soft magnet at vanishing applied fields and (ii) the case of a nearly saturated texture-free ferromagnet. In (i), the vector  $\mathbf{m}$  takes on all orientations with equal probability, and independent of the orientation of  $\mathbf{q}$ , whereas in (ii) the vector  $\mathbf{m}$  is confined to the plane normal to  $\langle \mathbf{M} \rangle$ , with a constant expectation value independent of the orientation of  $\mathbf{q}$ . In both cases  $C$  is isotropic,  $C = C(r)$ , and

$$C(r) = 4\pi V^{-1} r^{-1} \int_{q=0}^{\infty} q m^2(q) \sin(qr) dq. \quad (3)$$

The scattering cross-section due to the static spin misalignment is (6)

$$\frac{d\bar{\Sigma}_M}{d\Omega}(\mathbf{q}) = \frac{8\pi^3}{V} b_{\text{mag}}^2 \rho_a^2 |\mathbf{m}(\mathbf{q})|^2 \sin^2 \alpha, \quad (4)$$

where  $\alpha$  denotes the angle included by  $\mathbf{m}$  and  $\mathbf{q}$ ,  $b_{\text{mag}}$  is the atomic magnetic scattering length, and  $\rho_a$  the atomic density. We have computed the appropriate averages of  $\sin^2 \alpha$  over the allowed orientations of  $\mathbf{m}$  and  $\mathbf{q}$ , and have solved the resulting equation for the radial average scattering cross section,  $d\bar{\Sigma}_M/d\Omega$  for  $m^2(q)$ . Substituting the result in Eq. (3) yields

$$C(r) = a(2\pi^2 b_{\text{mag}}^2 \rho_a^2 r)^{-1} \int_{q=0}^{\infty} q \frac{d\bar{\Sigma}_M}{d\Omega}(q) \sin(qr) dq, \quad (5)$$

with  $a = 3/2$  and  $a = 16/(3\bar{g})$  for case (i) and (ii), respectively. In spite of the quite different orientation-distributions of  $\mathbf{m}$  these results agree to within less than  $\pm 10\%$ . In our data analysis we used an average value,  $a = 1.6$ .

A correlation length,  $l_C$ , of the spin misalignment is defined by  $l_C = -1/[d\ln(C)/dr]|_{r \rightarrow 0}$ . In particular, this definition yields  $l_C$  when the correlation decays exponentially,  $C(r) \propto \exp(-r/l_C)$ .

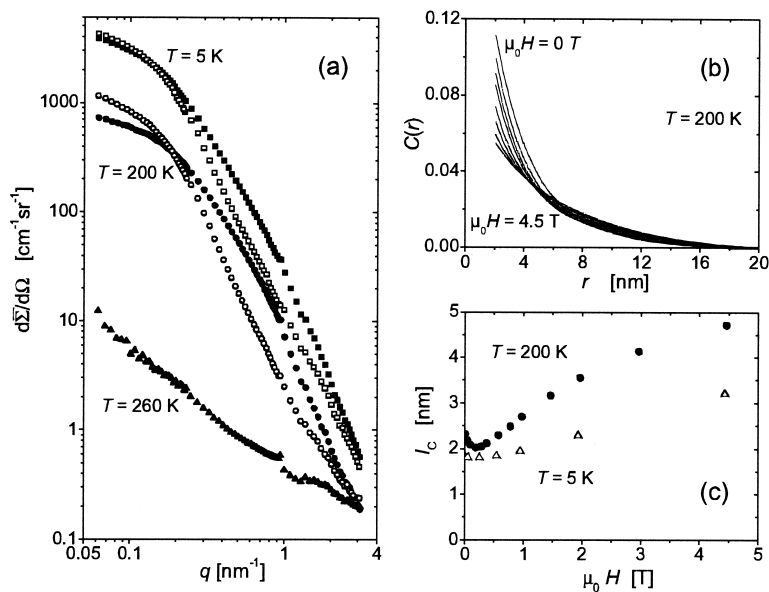


Figure 1. (a) Experimental differential scattering cross-section  $d\bar{\Sigma}/d\Omega$  versus modulus  $q$  of the scattering vector for applied magnetic fields  $\mu_0 H = 0$  (closed symbols) and  $\mu_0 H = 4.5\text{ T}$  (open symbols). (b) Correlation function  $C(r)$  at  $T = 200\text{ K}$  and at various  $H$ . (c) Correlation length  $l_c$  versus applied field  $H$  at  $T = 5\text{ K}$  and  $T = 200\text{ K}$ .

### Experimental Results and Discussion

The bulk sample of nanocrystalline Tb was prepared by the inert-gas condensation and consolidation method. X-ray diffraction shows that the material is hcp and a mean grain size of  $D = 9 \pm 2\text{ nm}$  is obtained by analysis of the integral widths of the Bragg reflections, correcting for microstrain broadening. Archimedes density measurement yields  $95 \pm 3\%$  of the literature value for conventional coarse-grained Tb. Measurements of the macroscopic magnetization with a vibrating sample magnetometer at temperatures between  $10\text{ K}$  and  $T_C$  show that the sample cannot be saturated with applied fields of  $9\text{ T}$ . The coercive field was found to be  $530\text{ mT}$  ( $54\text{ mT}$ ) at  $T = 10\text{ K}$  ( $200\text{ K}$ ), and AC-susceptometry indicates that the Curie temperature is  $T_C = 223.2\text{ K}$ , close to the literature value of  $220\text{ K}$  (8).

The SANS experiments were carried out with an unpolarized beam of wavelength  $\lambda = 0.6\text{ nm}$  at instrument V4 at the Berlin Neutron Scattering Center (BENS) equipped with a  $5\text{ T}$  vertical field cryomagnet. The scattering data was corrected in the usual way for dark current and for the scattering by the cryostat windows, normalized with a water standard, and radially averaged. Figure 1 shows  $d\bar{\Sigma}/d\Omega$  at  $T = 5\text{ K}$  and  $200\text{ K}$  for applied magnetic fields  $\mu_0 H = 0$  and  $4.5\text{ T}$ . Also shown is  $d\bar{\Sigma}/d\Omega$  at  $\mu_0 H = 0$  and  $T = 260\text{ K}$ , in the paramagnetic state, where the experiment measures the nuclear scattering cross section due to the porosity. It is seen, that at all fields the scattering cross-section in the ferromagnetic state is considerably higher than that in the paramagnetic state and is therefore dominated by the magnetic scattering, whereas the nuclear contribution is small. It is also seen, that the effect of increasing  $H$  on the scattering cross section is dramatically different from the case of soft magnets, where applied fields of  $2\text{ T}$  have been found to align the magnetization with the field direction, thereby reducing the magnetic scattering by several orders of magnitude (2,4). By comparison,  $d\bar{\Sigma}/d\Omega$  in Tb is seen to depend only weakly on  $H$ , indicating that the maximum applied field of  $4.5\text{ T}$  is insufficient to align the spins. What is more, the scattering curves exhibit a ‘cross-over’ at about  $q = 0.2\text{ nm}^{-1}$ , in

other words, increasing  $H$  has the quite counterintuitive effect to increase the scattering contrast at small  $q$ .

We compute the pore scattering in the ferromagnetic state based on the 260 K data, correcting for the change in the combined nuclear and magnetic scattering cross-section of a pore when the surrounding material orders ferromagnetically. This data was subtracted from the  $d\bar{\Sigma}/d\Omega$  at  $T < T_C$  to obtain the magnetic scattering cross-section due to the spin misalignment,  $d\bar{\Sigma}/d\Omega$ , and the correlation function computed by combining  $d\bar{\Sigma}/d\Omega$  with Eq. (5). Fig. 1b shows  $C(r)$  at  $T = 200$  K. The correlation is seen to exhibit a strongly field-dependent decay at small  $r$ . We have estimated the correlation length from the logarithmic derivative of  $C(r)$  in the limit of small  $r$ . For the 200 K data the result, Fig. 1c, shows that after an initial drop  $l_C$  increases, from its minimum value of 2.6 nm to 5.3 nm at  $\mu_0 H = 4.5$  T. At  $T = 5$  K  $l_C$  is even smaller, with a weaker field-dependence and with minimum a value close to the experimental resolution of about 2 nm.

If the spins were aligned in parallel within each grain then, for idealized spherical grains (9),  $C(r) = 1 - 3r/2D + r^3/2D^3$  and, hence,  $l_C = 2D/3$ , or  $l_C = 6$  nm for the experimental grain size. At  $T = 200$  K this value agrees with the experimental  $l_C$  at large applied field, indicating that the moments in each individual crystallite are nearly aligned in parallel at  $\mu_0 H = 4.5$  T. At this field, the scattering cross section is large, indicating strong misalignment of moments. In Tb, the ‘easy axes’ of the magnetization are in the hexagonal basal plane and a large applied field, about 20 T (8), is required to align the magnetization with the c-axes, suggesting that the net magnetization of each particle remains locked in to the hexagonal basal plane. When the field is reduced,  $l_C$  decreases, indicating that the magnetization gets less uniform *within* each grain. Since the in-plane anisotropy of Tb is much weaker than the out-of-plane one this suggests that across a particle the in-plane orientation of  $\mathbf{M}$  varies. This is somewhat similar to the helical spin structure of antiferromagnetic Tb, but without the crystallographic order. A likely origin for the internal structure in the nanocrystalline material is a ‘frustrated exchange’ interaction with the magnetization in the various neighboring grains of different crystallographic orientation. At  $T = 5$  K, higher applied fields are required to overcome the stronger exchange interaction and the higher in-plane anisotropy, hence  $l_C$  has a weaker field-dependence.

A final comment relates to the unusual ‘cross-over’ of the scattering curves. The most obvious effect of an increased applied magnetic field on the magnetization is to align all the spins more parallel, thereby reducing  $d\bar{\Sigma}/d\Omega$ , contrary to what we observed at small  $q$ . We have argued that the field induces little re-alignment for the long-wavelength (small  $q$ ) fluctuations because the net orientations of moments on a scale of the grain size and on larger scales are fixed, locked in to the basal planes of each grain. However, as the moments inside each individual particle are progressively aligned by the applied field the *magnitude* of the net magnetization of each particle increases, and thereby the scattering contrast is enhanced even though the *misalignment* of the net moment remains a constant. When the orientations are fixed then this latter effect dominates the field-dependence of the scattering pattern, and leads to the observed increase of  $d\bar{\Sigma}/d\Omega$  with increasing magnetic field.

### Acknowledgment

Support by the Deutsche Forschungsgemeinschaft (Heisenberg program and SFB 277) is gratefully acknowledged.

### References

1. W. Wagner, A. Wiedenmann, W. Petry, A. Geibel, and H. Gleiter, J. Mater. Res. 6, 2305 (1991).
2. J. Weissmüller, R. D. McMichael, J. G. Barker, H. J. Brown, U. Erb, and R. D. Shull, MRS Proc. 457, 231 (1997).

3. J. Löffler, G. Kostorz, A. Wiedenmann, and W. Wagner, *Phys. B.* 241–3, 603 (1998).
4. A. Michels, J. Weissmüller, A. Wiedenmann, and J. G. Barker, *J. Appl. Phys.* 87 5953 (2000); A. Michels, J. Weissmüller, A. Wiedenmann, J. S. Pedersen, and J. G. Barker, *Phil. Mag. Lett.* 80, 785 (2000).
5. J. Kohlbrecher, A. Wiedenmann, and H. Wollenberger, *Z. Phys. B.* 104, 1 (1997).
6. J. Weissmüller, R. D. McMichael, A. Michels, and R. D. Shull, *J. Res. NIST.* 104, 261 (1999).
7. J. Weissmüller, A. Michels, and D. Michels, in preparation.
8. J. L. Féron, G. Hug, and R. Pauthenet, *Z. Angew. Phys.* 30, 61 (1970).
9. G. Porod, in *Small-Angle X-ray Scattering*, ed. O. Glatter and O. Krattky, sect. 2, Academic Press, London (1982).